

A study of the bosonic sector of the two-dimensional Hubbard model within a two-pole approximation

Adolfo Avella,^{*} Ferdinando Mancini,[†] and Volodymyr Turkowski[‡]
Dipartimento di Fisica “E.R. Caianiello” - Unità INFM di Salerno
Università degli Studi di Salerno, I-84081 Baronissi (SA), Italy

(Dated: March 23, 2022)

The charge and spin dynamics of the two-dimensional Hubbard model in the paramagnetic phase is first studied by means of the two-pole approximation within the framework of the Composite Operator Method. The fully self-consistent scheme requires: no decoupling, the fulfillment of both Pauli principle and hydrodynamics constraints, the simultaneous solution of fermionic and bosonic sectors and a very rich momentum dependence of the response functions. The temperature and momentum dependencies, as well as the dependency on the Coulomb repulsion strength and the filling, of the calculated charge and spin susceptibilities and correlation functions are in very good agreement with the numerical calculations present in the literature.

PACS numbers: 71.27, 71.10.f

I. INTRODUCTION

The Hubbard model^{1,2,3} is capable to describe a rich variety of behaviors including a wide range of different spin and charge dynamics⁴. In particular, its interactions are thought to be responsible for strong antiferromagnetic correlations at half-filling and low temperatures⁵. In the presence of doping, the antiferromagnetic correlations remain rather strong although the correlation length can get smaller and smaller on increasing the doping. The possibility of charge order and phase separation has also been widely investigated according to the fact that one of the mostly used derivative of the Hubbard model, the t-J model, seems to present charge separation for a wide range of external parameters⁶. However, recent numerical results seems to indicate that the two models may have different behavior as far as charge correlations are concerned⁷.

In this manuscript, we first give a fully self-consistent treatment of the charge and spin dynamics of the two-dimensional Hubbard model in the two-pole approximation within the framework of the Composite Operator Method (COM)^{8,9}. The fermionic and bosonic sectors are solved together self-consistently, no decoupling approximation is used and the explicit momentum dependence of the spectra involves third nearest-neighbor sites that forces a rather complex and rich momentum dependence in all physical properties.

The COM rightfully belongs to the family of the projection methods^{10,11,12,13,14,15,16,17,18,19,20,21,22,23,24,25,26,27,28,29,30,31,32,33,34,35,36,37,38,39,40,41,42,43,44,45,46,47,48,49,50,51,52,53,54,55,56,57,58,59,60,61,62,63,64,65,66,67,68,69,70,71,72,73,74,75,76,77,78,79,80,81,82,83,84,85,86,87,88,89,90,91,92,93,94,95,96,97,98,99,100} and is based on two main ideas¹: strongly interacting systems should be described in terms of the quasi-particles generated by the interactions and the dynamics should be bounded to the right Hilbert space through the imposition of constraints coming from the Pauli principle. By Pauli principle we mean all the relations among operators dictated by the algebra². With respect to other projection methods the COM has some distinguishable peculiarities. In particular, within the COM, there is an absolute freedom to choose, as asymptotic fields, those

that are most suitable with respect to the properties of the system we wish to describe. This means that we are not bound to any specific recipe to choose them and that we can use this freedom to exploit at will the benefits coming from one choice or another. We can reproduce the results of the other methods in an unique framework and also go well beyond. For instance, by choosing suitable asymptotic fields and the closure of their equations of motion, we were able to describe the lowest energy scale, which is not algebraic in the model parameters, of impurity models³⁹. This result is absolutely precluded to other projection methods that uniquely focus on the preservation of spectral moments of higher and higher order. According to this, the method is continuously developing as we are constantly seeking, one system after the other, both the most suitable asymptotic fields and the most effective procedures to determine self-consistently the dynamics.

Once the fermionic propagator is known there are several ways to compute the response functions (i.e., the retarded propagators of the two-particle excitations: charge, spin, pair, ...). Many techniques are related to the possible diagrammatic expansions of the two-particle propagators in terms of the single-particle one (i.e., the fermionic propagator). However, when operators with non-canonical commutations are involved the only feasible approach is based on the one-loop approximation. The complicated algebra of the composite operators invalidates the Wick theorem and, consequently, does not allow any simple extension of decoupling schemes and more involved diagrammatic approximations^{40,41}. According to this, we have developed and widely applied a standard procedure to use, by means of the equations of motion approach, the one-loop approximation for composite operators⁴².

In this manuscript, we consider another way to tackle the problem: the two-particle excitations can be considered as a new sector in the dynamics of the system and we can choose also for them a suitable asymptotic basis alike it has been done for the fermions. This gives a new set of

equations obeyed by the two-particle Green's functions and the appearance of zero-frequency constants and unknown correlators. Also in this case, the enforcement of the constraints deriving from the Pauli principle allows to compute all the parameters and to fix the representation of the Hilbert space[?].

Within the framework of the *COM*, both methods have advantages and disadvantages. The one-loop approximation becomes exact in the non-interacting limit, well describes the incoherent behavior of the two-particle propagators and establishes a tight connection between the one- and two-particle propagators. These are really relevant properties once we wish to describe the bosonic excitations starting from its fundamental constituents: the electrons. The Fermi surface bending and nesting and the position of the van Hove singularities strongly influence the charge and spin response functions. According to this, we managed to give an explanation for the spin magnetic incommensurability issue[?] and the overdoped transition of the cuprate superconductors[?]. On the other hand, the one-loop approximation is not adequate to describe the system in the proximity of ordered phases as the dynamics of the bosonic excitations is mainly described in terms of *scattering* of elementary electronic excitations. This practically induces so strong finite life-time effects to prevent any possible softening of the bosonic modes. As discussed in the above, any possible extension involves so complicated diagrammatic expansions to be practically unfeasible.

As regards the pole approximation for the two-particle propagators we have obvious advantages like: the possibility to easily get the spectra and the analytical expressions of correlation functions and susceptibilities; the capability to study instabilities (i.e., the softening of the modes) in the whole range of model and external parameters; the possibility to consider the bosonic excitations as the media of new interactions among the electrons. In this paper, we show that it is possible to get spin antiferromagnetic correlations and weak charge ordering tendency at commensurate filling in exceptionally good agreement with the numerical results present in the literature. On the other hand, the pole approximation is based on a description of the bosonic excitations as true quasi-particles: the two-particle properties are entirely controlled by the dynamics, which is only weakly *renormalized* by the fermions; the single-particle properties (e.g., Fermi surface shape, position of the van Hove singularity, ...) do not influence significantly the response function behaviors; the finite life-time effects are completely neglected and the tendency towards ordering (i.e., softening) is sometime exaggerated. Anyway, the use of the Green's function formalism for the bosonic sector opens the possibility to explore another really relevant issue: the ergodicity of the bosonic dynamics and the presence of zero-frequency constants in the expression of the casual Green's function and of the correlation functions[?]. In this manuscript, we decided not to pursue this analysis and to fix the zero-frequency con-

stant values by means of ergodicity requirements in accordance with the general understanding of bulk systems.

As we can see, the two methods are effectively complementary and can be used to describe the spin and charge dynamics of the system in different region of the parameter space according to the relevance and prevalence of localization and ordering (two-pole) with respect to delocalization and symmetry (one-loop).

It is also worth noting that the pole approximation allows, at least in principle, to get a completely self-consistent solution putting together fermionic, spin, charge and pair propagators[?]. The Pauli principle could be then used to get also the zero-frequency constants in self-consistency and definitely fix the Hilbert space, as described in Ref. ? .

II. THE HUBBARD MODEL AND THE FERMIONIC SECTOR

The Hubbard model is described by the following Hamiltonian

$$H = \sum_{\mathbf{ij}} (t_{\mathbf{ij}} - \mu \delta_{\mathbf{ij}}) c^\dagger(i) c(j) + U \sum_{\mathbf{i}} n_\uparrow(i) n_\downarrow(i) \quad (2.1)$$

where $c^\dagger(i) = \begin{pmatrix} c^\dagger_\uparrow(i) \\ c^\dagger_\downarrow(i) \end{pmatrix}$ is the electronic creation operator in spinorial notation at the site $\mathbf{i} [i = (\mathbf{i}, t)]$ and $n_\sigma(i) = c^\dagger_\sigma(i) c_\sigma(i)$ is the number operator for spin σ at the site \mathbf{i} ; μ is the chemical potential and U is the on-site Coulomb repulsion.

The matrix $t_{\mathbf{ij}}$ describes the nearest-neighbor hopping; in the 2D case we have $t_{\mathbf{ij}} = -4t \alpha_{\mathbf{ij}}$, where

$$\alpha_{\mathbf{ij}} = \frac{1}{N} \sum_{\mathbf{k}} e^{i\mathbf{k}(\mathbf{i}-\mathbf{j})} \alpha(\mathbf{k}) \quad (2.2)$$

is the projector on the nearest-neighbor sites and $\alpha(\mathbf{k}) = \frac{1}{2} [\cos(k_x a) + \cos(k_y a)]$ and a is the lattice parameter.

We choose the following fermionic basis[?] ? ?

$$\Psi(i) = \begin{pmatrix} \xi(i) \\ \eta(i) \end{pmatrix} \quad (2.3)$$

where $\xi(i) = [1 - n(i)] c(i)$ and $\eta(i) = n(i) c(i)$ are the Hubbard operators. $\Psi(i)$ satisfies the following equation of motion

$$J(i) = i \frac{\partial}{\partial t} \Psi(i) = \begin{pmatrix} -\mu \xi(i) - 4t c^\alpha(i) - 4t \pi(i) \\ -(\mu - U) \eta(i) + 4t \pi(i) \end{pmatrix} \quad (2.4)$$

where $c^\gamma(\mathbf{i}, t) = \sum_{\mathbf{j}} \gamma_{\mathbf{ij}} c(\mathbf{j}, t)$ [$\gamma_{\mathbf{ij}}$ stands for any projector on the \mathbf{j} neighbor sites of \mathbf{i} ; see Appendix] and $\pi(i) = \frac{1}{2} \sigma^\mu n_\mu(i) c^\dagger(i) + c(i) [c^{\dagger\alpha}(i) c(i)]$. $n_\mu(i) = c^\dagger(i) \sigma_\mu c(i)$ are the charge ($\mu = 0$) and spin ($\mu = 1, 2, 3$) density

operators, with $\sigma_\mu = (1, \vec{\sigma})$, $\sigma^\mu = (-1, \vec{\sigma})$ and $\vec{\sigma}$ are the Pauli matrices.

Let us project the source $J(i)$ on the chosen basis

$$J(\mathbf{i}, t) \cong \sum_{\mathbf{j}} \varepsilon(\mathbf{i}, \mathbf{j}) \Psi(\mathbf{j}, t) \quad (2.5)$$

Accordingly, the energy matrix $\varepsilon(\mathbf{i}, \mathbf{j})$ is defined through the equation

$$m(\mathbf{i}, \mathbf{j}) = \sum_{\mathbf{l}} \varepsilon(\mathbf{i}, \mathbf{l}) I(\mathbf{l}, \mathbf{j}) \quad (2.6)$$

where the m -matrix and the normalization matrix I have the following definitions

$$m(\mathbf{i}, \mathbf{j}) = \langle \{J(\mathbf{i}, t), \Psi^\dagger(\mathbf{j}, t)\} \rangle \quad (2.7)$$

$$I(\mathbf{i}, \mathbf{j}) = \langle \{ \Psi(\mathbf{i}, t), \Psi^\dagger(\mathbf{j}, t) \} \rangle \quad (2.8)$$

It is worth pointing out that in Eq. (2.7) $J(i)$ is the total current given in Eq. (2.4) and not the approximated one. After Eq. (2.5), the Fourier transform of the thermal single-particle retarded Green's function $G(i, j) = \langle R[\Psi(i) \Psi^\dagger(j)] \rangle$ satisfies the following equation

$$[\omega - \varepsilon(\mathbf{k})] G(\mathbf{k}, \omega) = I(\mathbf{k}) \quad (2.9)$$

The straightforward application of this scheme^{???} gives that, in the paramagnetic phase, $I(\mathbf{k})$ has diagonal form with $I_{11} = 1 - n/2$ and $I_{22} = n/2$ ($\langle n_\sigma(i) \rangle = \frac{n}{2}$) and that the m -matrix depends on three parameters: the chemical potential μ and two correlators

$$\Delta = \langle \xi^\alpha(i) \xi^\dagger(i) \rangle - \langle \eta^\alpha(i) \eta^\dagger(i) \rangle \quad (2.10)$$

$$p = \frac{1}{4} \langle n_\mu^\alpha(i) n_\mu(i) \rangle - \langle [c_\uparrow(i) c_\downarrow(i)]^\alpha c_\downarrow^\dagger(i) c_\uparrow^\dagger(i) \rangle \quad (2.11)$$

The three parameters μ , Δ and p are functions of the external parameters n , T and U and can be determined self-consistently through a set of three coupled equations

$$\begin{cases} n = 2 [1 - \langle c(i) c^\dagger(i) \rangle] \\ \Delta = \langle \xi^\alpha(i) \xi^\dagger(i) \rangle - \langle \eta^\alpha(i) \eta^\dagger(i) \rangle \\ \langle \xi(i) \eta^\dagger(i) \rangle = 0 \end{cases} \quad (2.12)$$

The first equation fixes the particle number, the second one comes from the definition of Δ and the third one assures that the solution respects the Pauli principle (i.e., the local algebra)[?]. In this latter equation resides the main difference with all the other two-pole approximations. This equation: allows to fix the representation[?]; implements the particle-hole symmetry in the solution[?]; avoids uncontrolled decoupling or further approximations on higher order correlators. Using this procedure is possible to find two solutions: one with a p positive and of order of the filling n and another with p mainly negative and rather small. The main difference between these two

solutions resides in the strength of the antiferromagnetic correlations^{??}.

It is worth noting that this set of coupled self-consistent equations gives the exact solution in the atomic and in the non-interacting cases as well as for the interacting two-site system[?]. According to this, we are confident to reproduce at least the two most relevant scale of energies in the system: the Coulomb repulsion U and the exchange energy J . The latter is already well defined on the two-site system that is the minimal cluster where J becomes effective.

Within this calculation scheme, the fermionic solution is known in a fully self-consistent manner and without opening the bosonic sector. Once we have the electronic Green's function we can get all single-particle, local and thermodynamic properties straightforwardly. In the last years, by means of the *COM* in the above described approximation, we got results in excellent agreement with numerical and exact solutions as regards many lattice and impurity systems^{????????????????}.

III. CHARGE AND SPIN RESPONSE PROPERTIES

As stated in the introduction we choose to compute the charge and spin response functions by studying the causal Green's function[?] $G^{(\mu)}(i, j) = \langle T[n_\mu(i) n_\mu(j)] \rangle$. As we widely discussed in Ref. [?], to obtain a correct description of the bosonic properties is necessary to compute first the causal Green's function and then derive from this latter all other propagators and correlators. The reason of this lies in the fact that the zero-frequency constants do not explicitly contribute to the retarded functions, although there is an implicit dependence through the self-consistent determination of the internal parameters. Starting from the retarded function would lead to ignore the zero-frequency constants and will give **wrong results**. Once we know the Fourier transform of $G^{(\mu)}(i, j)$, that is $G^{(\mu)}(\mathbf{k}, \omega)$, we can find spin and charge susceptibilities $\chi^{(\mu)}(\mathbf{k}, \omega) = -F \langle R[n_\mu(i) n_\mu(j)] \rangle$ and correlation functions $C^{(\mu)}(\mathbf{k}, \omega) = F \langle n_\mu(i) n_\mu(j) \rangle$ by means of the well-known formulas

$$\Re[\chi^{(\mu)}(\mathbf{k}, \omega)] = -\Re[G^{(\mu)}(\mathbf{k}, \omega)] \quad (3.1)$$

$$\Im[\chi^{(\mu)}(\mathbf{k}, \omega)] = -\tanh \frac{\omega}{2T} \Im[G^{(\mu)}(\mathbf{k}, \omega)] \quad (3.2)$$

$$C^{(\mu)}(\mathbf{k}, \omega) = -\left(1 + \tanh \frac{\omega}{2T}\right) \Im[G^{(\mu)}(\mathbf{k}, \omega)] \quad (3.3)$$

where T , R and F are the causal and retarded operators and the Fourier transform, respectively.

As widely discussed in the introduction, in this manuscript we will study the spin and charge channels of the bosonic sector by using a pole approximation. Let us write the equation of motion for the operator $n_\mu(i)$

$$i \frac{\partial}{\partial t} n_\mu(i) = -4t \rho_\mu(i) \quad (3.4)$$

where

$$\rho_\mu(i) = c^\dagger(i) \sigma_\mu c^\alpha(i) - c^{\dagger\alpha}(i) \sigma_\mu c(i) \quad (3.5)$$

The bosonic basis has to be chosen in order to be compatible with the fermionic one and with a non-local component as we wish to take into account, at least partially, the delocalization driven by the kinetic term of the Hamiltonian. According to this, the most natural choice is a two-component basis and, in particular, that directly generated by the hierarchy of the equations of motion. This will assure that the first four bosonic spectral moments have the correct functional form[?]. Therefore, we take as bosonic basis the following one

$$N_\mu(i) = \begin{pmatrix} n_\mu(i) \\ \rho_\mu(i) \end{pmatrix} \quad (3.6)$$

The equation of motion of $\rho_\mu(i)$ is the following one

$$i \frac{\partial}{\partial t} \rho_\mu(i) = -4t l_\mu(i) + U \kappa_\mu(i) \quad (3.7)$$

where the higher-order bosonic operators are defined by

$$\begin{aligned} \kappa_\mu(i) &= c^\dagger(i) \sigma_\mu \eta^\alpha(i) - \eta^\dagger(i) \sigma_\mu c^\alpha(i) \\ &\quad + \eta^{\dagger\alpha}(i) \sigma_\mu c(i) - c^{\dagger\alpha}(i) \sigma_\mu \eta(i) \end{aligned} \quad (3.8)$$

$$\begin{aligned} l_\mu(i) &= c^\dagger(i) \sigma_\mu c^{\alpha^2}(i) + c^{\dagger\alpha^2}(i) \sigma_\mu c(i) \\ &\quad - 2c^{\dagger\alpha}(i) \sigma_\mu c^\alpha(i) \end{aligned} \quad (3.9)$$

and the definition of $c^{\alpha^2}(i)$ can be found in Appendix.

Using the same procedure used for the fermions, we have

$$i \frac{\partial}{\partial t} N_\mu(\mathbf{i}, t) \cong \sum_{\mathbf{j}} \varepsilon^{(\mu)}(\mathbf{i}, \mathbf{j}) N_\mu(\mathbf{j}, t) \quad (3.10)$$

where $\varepsilon^{(\mu)}(\mathbf{i}, \mathbf{j})$ is given by

$$m^{(\mu)}(\mathbf{i}, \mathbf{j}) = \sum_{\mathbf{l}} \varepsilon^{(\mu)}(\mathbf{i}, \mathbf{l}) I^{(\mu)}(\mathbf{l}, \mathbf{j}) \quad (3.11)$$

and the normalization matrix $I^{(\mu)}$ and the $m^{(\mu)}$ -matrix have the following definitions

$$I^{(\mu)}(\mathbf{i}, \mathbf{j}) = \langle [N_\mu(\mathbf{i}, t), N_\mu^\dagger(\mathbf{j}, t)] \rangle \quad (3.12)$$

$$m^{(\mu)}(\mathbf{i}, \mathbf{j}) = \left\langle \left[i \frac{\partial}{\partial t} N_\mu(\mathbf{i}, t), N_\mu^\dagger(\mathbf{j}, t) \right] \right\rangle \quad (3.13)$$

As it can be easily verified, in the paramagnetic phase the normalization matrix $I^{(\mu)}$ does not depend on the index μ ; charge and spin operators have the same weight. The two matrices $I^{(\mu)}$ and $m^{(\mu)}$ have the following form in momentum space[?]

$$I^{(\mu)}(\mathbf{k}) = \begin{pmatrix} 0 & I_{12}^{(\mu)}(\mathbf{k}) \\ I_{12}^{(\mu)}(\mathbf{k}) & 0 \end{pmatrix} \quad (3.14)$$

$$m^{(\mu)}(\mathbf{k}) = \begin{pmatrix} m_{11}^{(\mu)}(\mathbf{k}) & 0 \\ 0 & m_{22}^{(\mu)}(\mathbf{k}) \end{pmatrix} \quad (3.15)$$

where

$$I_{12}^{(\mu)}(\mathbf{k}) = 4[1 - \alpha(\mathbf{k})] C^\alpha \quad (3.16)$$

$$m_{11}^{(\mu)}(\mathbf{k}) = -4t I_{12}^{(\mu)}(\mathbf{k}) \quad (3.17)$$

$$m_{22}^{(\mu)}(\mathbf{k}) = -4t I_{l_\mu \rho_\mu}(\mathbf{k}) + U I_{\kappa_\mu \rho_\mu}(\mathbf{k}) \quad (3.18)$$

The exact expressions of the normalization matrix entries and the definition of the parameters they depend on can be found in the Appendix. The energy matrix $\varepsilon^{(\mu)}(\mathbf{k})$ has off-diagonal form with non-zero elements

$$\varepsilon_{12}^{(\mu)}(\mathbf{k}) = -4t \quad (3.19)$$

$$\varepsilon_{21}^{(\mu)}(\mathbf{k}) = \frac{m_{22}^{(\mu)}(\mathbf{k})}{I_{12}^{(\mu)}(\mathbf{k})} \quad (3.20)$$

For the sake of simplicity, we will now extend the previous used notation for the bosonic causal Green's function $G^{(\mu)}(i, j) = \langle T[n_\mu(i) n_\mu(j)] \rangle$ to the complete 2×2 matrixial one, that is, $G^{(\mu)}(i, j)$ is hereafter defined as $\langle T[N_\mu(i) N_\mu^\dagger(j)] \rangle$. We will also use the accordingly extended notation for the correlation function $C^{(\mu)}(i, j)$. They have then the following expressions

$$\begin{aligned} G^{(\mu)}(\mathbf{k}, \omega) &= -i \frac{(2\pi)^3}{a^2} \delta^{(2)}(\mathbf{k}) \delta(\omega) \Gamma_\mu \\ &\quad + \sum_{n=1}^2 \sigma^{(n, \mu)}(\mathbf{k}) \frac{1 + f_B(\omega)}{\omega - \omega_n^{(\mu)}(\mathbf{k}) + i\delta} \\ &\quad - \sum_{n=1}^2 \sigma^{(n, \mu)}(\mathbf{k}) \frac{f_B(\omega)}{\omega - \omega_n^{(\mu)}(\mathbf{k}) - i\delta} \end{aligned} \quad (3.21)$$

$$\begin{aligned} C^{(\mu)}(\mathbf{k}, \omega) &= \frac{(2\pi)^3}{a^2} \delta^{(2)}(\mathbf{k}) \delta(\omega) \Gamma_\mu \\ &\quad + 2\pi \sum_{n=1}^2 \delta[\omega - \omega_n^{(\mu)}(\mathbf{k})] [1 + f_B(\omega)] \sigma^{(n, \mu)}(\mathbf{k}) \end{aligned} \quad (3.22)$$

where Γ_μ is the zero-frequency constant[?] and $f_B(\omega) = \frac{1}{e^{\beta\omega} - 1}$ is the Bose-Einstein distribution function. In this manuscript, we will use the ergodic value (i.e., $\Gamma_{11\mu} = \delta_{\mu 0} n^2$) for the zero-frequency constant as explained in the introduction. The energy spectra are given by

$$\omega_n^{(\mu)}(\mathbf{k}) = (-)^n \omega^{(\mu)}(\mathbf{k}) \quad (3.23)$$

$$\omega^{(\mu)}(\mathbf{k}) = \sqrt{\varepsilon_{12}^{(\mu)}(\mathbf{k}) \varepsilon_{21}^{(\mu)}(\mathbf{k})} \quad (3.24)$$

and the spectral functions have the following expression

$$\sigma^{(n, \mu)}(\mathbf{k}) = \frac{1}{2} I_{12}^{(\mu)}(\mathbf{k}) \begin{pmatrix} \frac{\varepsilon_{12}^{(\mu)}(\mathbf{k})}{\omega_n^{(\mu)}(\mathbf{k})} & 1 \\ 1 & \frac{\varepsilon_{21}^{(\mu)}(\mathbf{k})}{\omega_n^{(\mu)}(\mathbf{k})} \end{pmatrix} \quad (3.25)$$

As it can be seen from the expressions given in Appendix, the Green's function and the correlation function depend on various parameters, static correlation functions, that must be self-consistently calculated. A subset of parameters, C^α , C^λ , C^μ , E^β and E^η , are of fermionic nature and can be computed through the fermionic Green's function. The *negative* p solution will be used in order to get enhanced antiferromagnetic correlations. The remaining parameters, a_μ , b_μ , c_μ and d_μ , are of bosonic nature, but they cannot be expressed in terms of the bosonic Green's function under study as they belong to higher order propagators. As in the fermionic sector, we can avoid studying complicated higher order propagators requiring the fulfillment of the Pauli principle and of other symmetry requirements. Four equations will be used to fix these parameters: one equation comes from the Pauli principle and other three from the general properties of the bosonic spectra $\omega_n^{(\mu)}(\mathbf{k})$ for small momenta (i.e., for $k \rightarrow 0$ where $k = \sqrt{k_x^2 + k_y^2}$). The Pauli principle[?] gives

$$\langle n(i) n(i) \rangle = n + 2D \quad (3.26a)$$

$$\langle n_k(i) n_k(i) \rangle = n - 2D \quad k = 1, 2, 3 \quad (3.26b)$$

where $D = \langle n_\uparrow(i) n_\downarrow(i) \rangle = \frac{n}{2} - \langle \eta(i) \eta^\dagger(i) \rangle$ is the double occupancy. From the continuity equation[?] it follows that

$$\lim_{k \rightarrow 0} \omega_n^{(\mu)}(\mathbf{k}) \cong c_n^{(\mu)} k^s \quad (3.27)$$

where $s \geq 1$ and $c_n^{(\mu)}$ is the *velocity*. Let us analyze the expression for $\omega_n^{(\mu)}(\mathbf{k})$. The function $m_{22}^{(\mu)}(\mathbf{k})$ at small k can be cast in the following form

$$m_{22}^{(\mu)}(\mathbf{k}) = m_0^{(\mu)} + m_1^{(\mu)}(ka)^2 + m_2^{(\mu)}(ka)^4 + m_3^{(\mu)}(ka)^4 \sin^2(2\phi_k) + O((ka)^6) \quad (3.28)$$

where $\phi_k = \arctan \frac{k_y}{k_x}$. The function $I_{12}^{(\mu)}(\mathbf{k})$ behaves as $(ka)^2 C^\alpha$ at small k . Therefore, to satisfy the continuity equation we must put

$$m_0^{(\mu)} = m_1^{(\mu)} = 0 \quad (3.29)$$

Moreover, as the susceptibility has to be single-value at $k = 0$ we have also to require that $m_3^{(\mu)} = 0$. The coefficients of $m_{22}^{(\mu)}(\mathbf{k})$ in the limit of small k have the following expressions (see Appendix)

$$m_0^{(\mu)} = U(-a_\mu + \frac{1}{4}b_\mu + \frac{1}{2}c_\mu + \frac{1}{4}d_\mu) \quad (3.30)$$

$$m_1^{(\mu)} = \frac{U}{4}(2a_\mu - c_\mu - d_\mu - 2D - 2E^\eta) \quad (3.31)$$

$$m_3^{(\mu)} = -\frac{3}{8}t(C^\alpha - 2C^\mu + C^\lambda) + \frac{U}{48}(a_\mu + c_\mu - 2d_\mu - D + 6E^\beta - 7E^\eta) \quad (3.32)$$

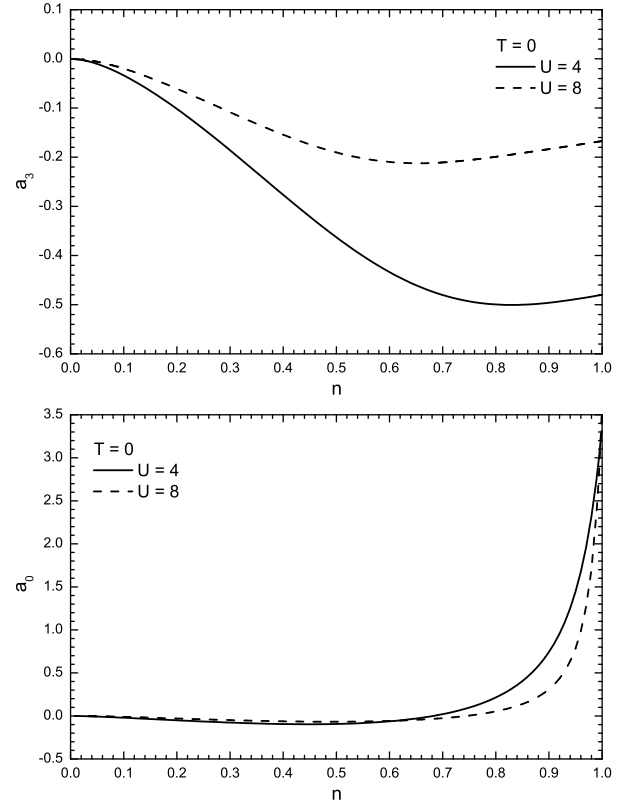


FIG. 1: a_3 and a_0 as functions of the filling n for $T = 0$ and $U = 4$ and 8 .

According to this, we can write the following algebraic relations for the parameters b_μ , c_μ and d_μ

$$b_\mu = a_\mu + 3D + E^\eta + 2E^\beta - 6\frac{t}{U}(C^\alpha + C^\lambda - 2C^\mu) \quad (3.33)$$

$$c_\mu = a_\mu - D + E^\eta - 2E^\beta + 6\frac{t}{U}(C^\alpha + C^\lambda - 2C^\mu) \quad (3.34)$$

$$d_\mu = a_\mu - D - 3E^\eta + 2E^\beta - 6\frac{t}{U}(C^\alpha + C^\lambda - 2C^\mu) \quad (3.35)$$

and use the Eq. (3.26) to compute the parameter a_μ self-consistently. In Fig. 1, we report the behavior of a_3 and a_0 as functions of the filling n for $T = 0$ and $U = 4$ and 8 . The behavior of a_3 reveals a strong dependence on both filling and Coulomb repulsion of the intensity of spin correlations. In particular, at half-filling we have the maximum dependence on U . a_0 , instead, is practically featureless except for a region near half filling, whose extension is controlled by the strength of the Coulomb repulsion, where rapidly and enormously increases with a slope that again depends on U . This latter behavior results in a strong enhancement of the charge correlations in the proximity of the Mott-Hubbard metal-insulator

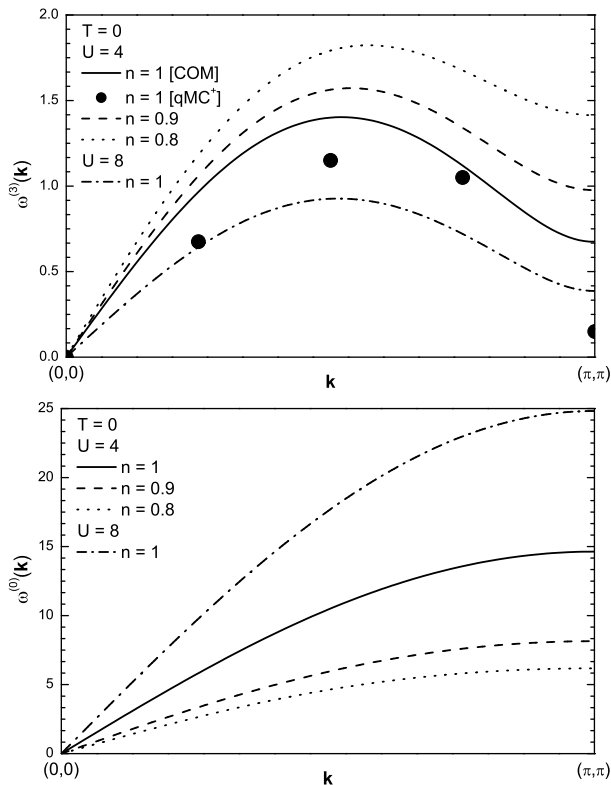


FIG. 2: The spin $\omega^{(3)}(\mathbf{k})$ and charge $\omega^{(0)}(\mathbf{k})$ spectra as functions of the momentum ($k_x = k_y$) for $n = 1, 0.9, 0.8$, $U = 4$ and 8 and $T = 0$; the qMC⁺ data (10×10) for $\omega^{(3)}(\mathbf{k})$ at $U = 4$, $n = 1$ and $T = 0$ are from ? .

transition.

It is necessary to report that this analysis can be considered an extension and a completion of that done in Ref. ? . The main differences are related to the use of causal propagator in place of the retarded one and to the exploitation of the hydrodynamics constraints to fix the parameters coming in the energy spectra whenever we wish to retain the complete dependence on the momentum.

IV. RESULTS

A. Spin and charge spectra

The spin and charge spectra, as functions of the momentum, are reported in Fig. 2 for $n = 1, 0.9, 0.8$, $U = 4$ and 8 and $T = 0$. As regards the spin spectrum, COM result is in fair agreement with the quantum Monte Carlo data[?] (10×10) except for $\mathbf{k} = (\pi, \pi) = \mathbf{Q}$. The very small value reported by the numerical data at \mathbf{Q} can be understood as a consequence of overestimated antiferromagnetic correlations (i.e., the antiferromagnetic correlation length actually exceeds the cluster size, see Fig. 9). COM results, instead, are obtained with paramagnetic

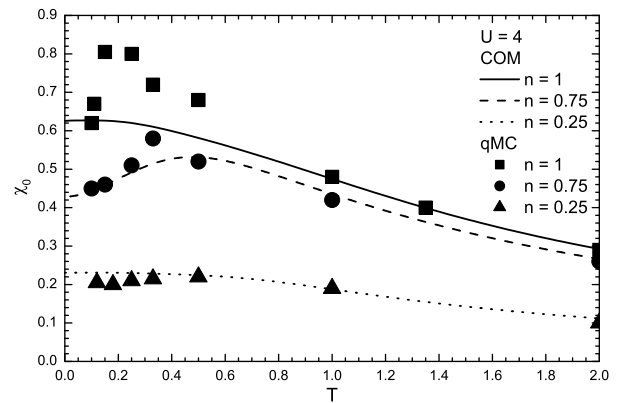


FIG. 3: The uniform static spin susceptibility χ_0 as function of the temperature T for $U = 4$, $n = 1, 0.75$ and 0.25 ; the qMC data (8×8) are from ? .

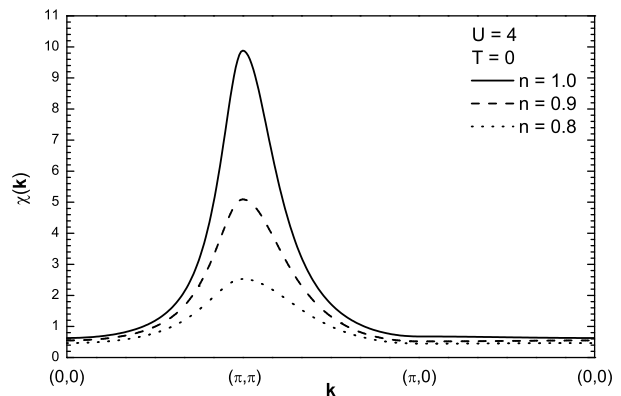


FIG. 4: The spin susceptibility $\chi(\mathbf{k})$ as function of the momentum for $U = 4$, $T = 0$ and $n = 1, 0.9$ and 0.8 .

boundary conditions. The minimum at \mathbf{Q} in the spin spectrum is the clearest possible evidence that we have quite strong antiferromagnetic correlations in our solution. The doping is quite efficient in reducing the intensity of them. On the contrary, they significantly increase with the Coulomb repulsion according to the stronger and stronger influence of the exchange energy J in the strongly interacting regime. The charge spectrum shows an enhancement of the *velocity* with decreasing doping and increasing Coulomb repulsion, that is, in the proximity of a Mott-Hubbard metal-insulator transition, which would have as signature the divergency of the former.

B. Spin susceptibility

The dynamical spin susceptibility $\chi_s(\mathbf{k}, \omega)$ can be obtained by Eqs. (3.1) and (3.2) with $\mu = 3$ and has the

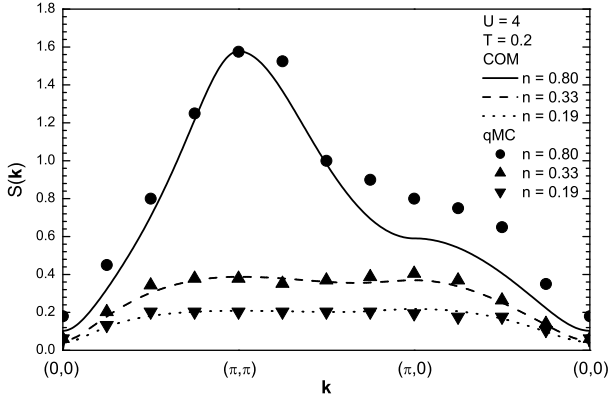


FIG. 5: The spin correlation function $S(\mathbf{k})$ as function of the momentum for $U = 4$, $T = 0.2$ and $n = 0.8, 0.33$ and 0.19 ; the qMC data (8×8) are from ? .

expression

$$\chi_s(\mathbf{k}, \omega) = - \sum_{n=1}^2 \frac{\sigma_{11}^{(n,3)}(\mathbf{k})}{\omega - \omega_n^{(3)}(\mathbf{k}) + i\delta} \quad (4.1)$$

According to this, the static $\chi(\mathbf{k}) = \lim_{\omega \rightarrow 0} \chi_s(\mathbf{k}, \omega)$ and the static and uniform $\chi_0 = \lim_{\mathbf{k} \rightarrow 0} \chi(\mathbf{k})$ spin susceptibility are given by

$$\chi(\mathbf{k}) = \frac{\{4[1 - \alpha(\mathbf{k})]C^\alpha\}^2}{m_{22}^{(3)}\mathbf{k}} \quad (4.2)$$

$$\chi_0 = - \frac{(4C^\alpha)^2}{24t(C^\alpha - C^\mu) - U(c_3 + 4E^\beta)} \quad (4.3)$$

χ_0 , as a function of the temperature, is reported in Fig. 2 for $U = 4$ and $n = 0.25, 0.75$ and 1 . *COM* results are in very good agreement with the quantum Monte Carlo ones⁷ (8×8) for $n = 0.25$ and 0.75 . For $n = 1$ and low temperatures, our paramagnetic solution cannot reproduce the overestimated antiferromagnetic correlations present in the numerical results. Anyway, our spin susceptibility $\chi(\mathbf{k})$ and our spin correlation function $S(\mathbf{k})$ (see next section) present a large enhancement at \mathbf{Q} on reducing the doping (see Fig. 4) and increasing the Coulomb repulsion (see Figs. 5 and 6) showing that also *COM* results present well developed antiferromagnetic correlations although they should be compatible with the chosen paramagnetic solution. It is worth noting that the presented results are in better agreement with quantum Monte Carlo data than the random phase approximation and the *COM* within the one-loop approximation (see Ref. ? and references therein).

C. Spin correlation function

The spin correlation function is defined as

$$S(\mathbf{i}, \mathbf{j}) = \langle n_3(\mathbf{i}, t) n_3(\mathbf{j}, t) \rangle = F^{-1}[S(\mathbf{k})] \quad (4.4)$$

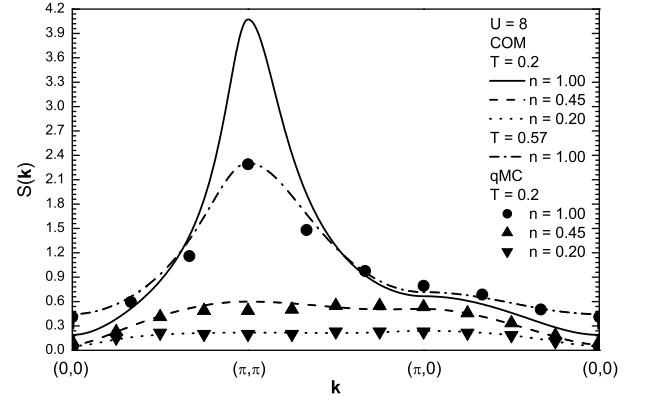


FIG. 6: The spin correlation function $S(\mathbf{k})$ as function of the momentum for $U = 8$, $T = 0.2$ and $T = 0.57$ and $n = 1, 0.45$ and 0.2 ; the qMC data (8×8) are from ? .

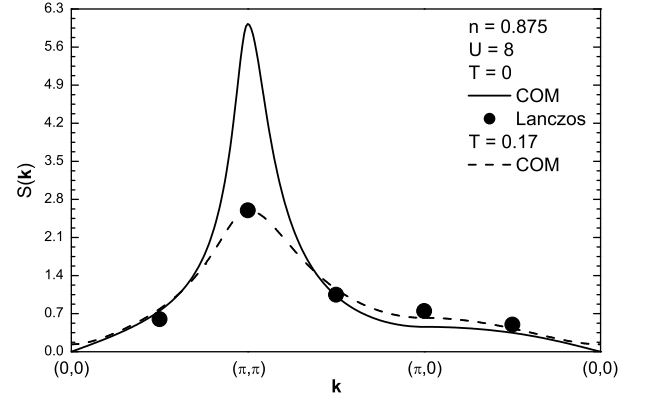


FIG. 7: The spin correlation function $S(\mathbf{k})$ as function of the momentum for $n = 0.875$, $U = 8$ and $T = 0$ and 0.17 ; the Lanczos data (4×4) at $T = 0$ are from ? .

where F^{-1} stands for the Fourier anti-transform and the structure factor reads as

$$S(\mathbf{k}) = - \frac{2t I_{12}^{(3)}(\mathbf{k})}{\omega^{(3)}(\mathbf{k})} \coth \frac{\omega^{(3)}(\mathbf{k})}{2T} \quad (4.5)$$

The behavior of $S(\mathbf{k})$, as function of the momentum, is reported in Figs. 5, 6 and 7 in comparison with some numerical data^{7, 8, 9} for different values of filling, Coulomb repulsion and temperature. We have a very good agreement with the numerical results for sufficiently high values of the doping for all shown values of the Coulomb repulsion. In the proximity of half-filling the numerical data suffer from a saturation of the antiferromagnetic correlation length⁷ that becomes comparable with the size of the cluster. For $U = 4$ and $n = 0.8$ (see Fig. 5), the correlation length is slightly smaller than the size of the cluster: our solution results capable to describe this situation fairly well (the height of the peak at \mathbf{Q} is exactly reproduced and the momentum dependence is

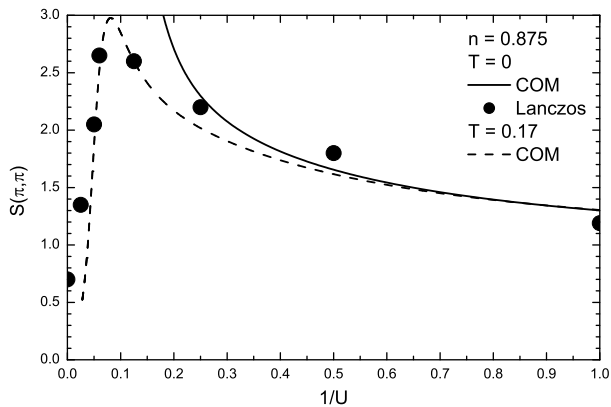


FIG. 8: The spin correlation function at \mathbf{Q} ($S(\mathbf{Q})$) as function of the inverse of U for $n = 0.875$ and $T = 0$ and 0.17 ; the Lanczos data (4×4) at $T = 0$ are from ? .

qualitatively correct, again practically exact along the diagonal) except for the exact value of the numerical data along the main axes. This is probably due again to an overestimation of the correlations by the numerical analysis owing to the finite size of the cluster. For $U = 8$ and $n = 1$ (see Fig. 6) and 0.875 (see Fig. 7), in order to reproduce the numerical data we need to increase the temperature as to decrease our value of the correlation length and match that of the numerical analysis, which is stuck at the saturation value due to the finiteness of the clusters. The results of such a procedure are astonishing, we manage to exactly reproduce the numerical data for any value of the momentum, and not only at \mathbf{Q} , revealing the correctness and power of our approach and the limitations of the numerical analysis. According to this, we wish to point out that the numerical data need to be carefully and cleverly interpreted in order to obtain from them sensible and effective information. The behavior of the spin correlation function as a function of $1/U \propto J$ (the exchange energy) is shown in Fig. 8. Again, in order to obtain results comparable with the numerical ones⁷ we need to use an higher temperature: at $T = 0$ and for high enough values of U , our results show a divergency in the correlation length that is extraneous to the physics of a finite system. By using the same temperature of Fig. 7 (the Lanczos data have the same source), we get a very good agreement for any regime of interaction: our solution properly describes also the low-energy dynamics of the spin system.

In Fig. 9, we report the behavior of $S(i, j)$ along the three principal directions in the lattice for $U = 4$, $T = 0.1$ and (top) $n = 1$ [(bottom) $n = 0.5$]. The quantum Monte Carlo results² at $n = 1$ present an antiferromagnetic correlation length as large as the size of the cluster. The correlation along the principal axes $[(0, 0) \rightarrow (i_x, 0)$ and $(5, 0) \rightarrow (5, i_y)]$ is antiferromagnetic and is ferromagnetic along the diagonals $[(0, 0) \rightarrow (i, i)]$ as in an ordinary two-dimensional Néel phase. COM results show

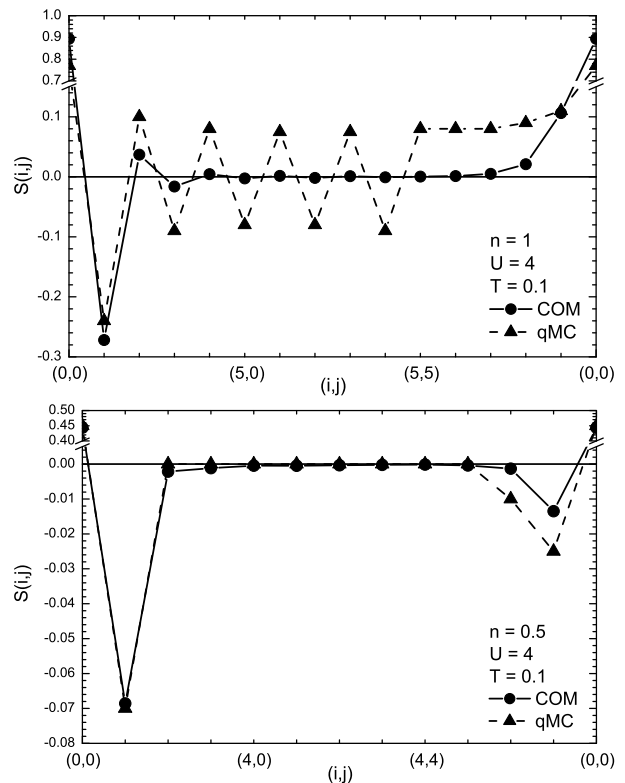


FIG. 9: The spin correlation function $S(i, j)$ along the principal directions for $U = 4$, $T = 0.1$ and (top) $n = 1$ [(bottom) $n = 0.5$]; the qMC data (10×10) are from ? .

exactly the same behavior although the correlation length is much smaller: we analyze the paramagnetic phase and for $U = 4$ we still not have so well developed antiferromagnetic correlations. The on-set of an antiferromagnetic phase (i.e., to have an antiferromagnetic correlation length as large as the size of the system) for a finite system seems possible for any finite value of U at half-filling, while, for an infinite system, it could be related to the existence of a critical value of the interaction U that, in our case, falls between 4 and 8. Actually, our study of the antiferromagnetic phase⁷ confirm that our critical value is $U_c \cong 6$. At $n = 0.5$ the agreement becomes quantitative as the strong antiferromagnetic correlations present at half filling completely disappear.

D. Charge correlation function

The charge correlation function is defined as

$$N(\mathbf{i}, \mathbf{j}) = \langle n(\mathbf{i}, t) n(\mathbf{j}, t) \rangle = F^{-1} [N(\mathbf{k})] \quad (4.6)$$

where $N(\mathbf{k})$ reads as

$$N(\mathbf{k}) = -\frac{2t I_{12}^{(0)}(\mathbf{k})}{\omega^{(0)}(\mathbf{k})} \coth \frac{\omega^{(0)}(\mathbf{k})}{2T} \quad (4.7)$$

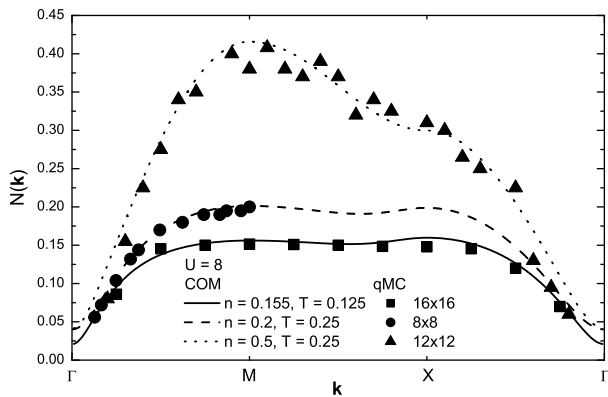


FIG. 10: The charge correlation function $N(\mathbf{k})$ as a function of the momentum for $U = 8$, $T = 0.125$ and 0.25 and $n = 0.155$, 0.2 and 0.5 ; the qMC data (8×8 , 12×12 , 16×16) are from ? .

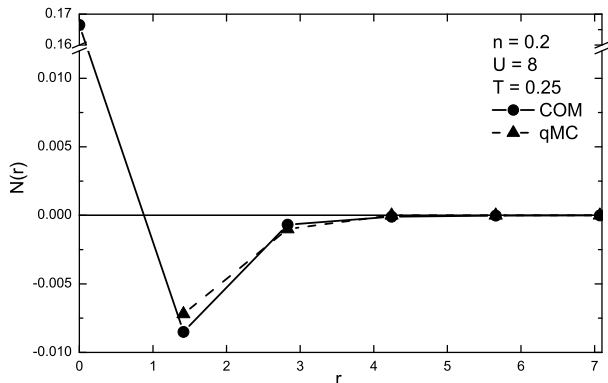


FIG. 11: The charge correlation function $N(r)$ as a function of the distance for $n = 0.2$, $U = 8$ and $T = 0.25$; the qMC data (16×16) are from ? .

$N(\mathbf{k})$ is reported in Fig. 10, as a function of the momentum, for various fillings and temperatures and $U = 8$. We have again a very good agreement with quantum Monte Carlo results⁷ for all shown values of the external parameters and of the momentum. The enhancement at $\mathbf{k} = \mathbf{Q} = M$ for $n = 0.5$ can be interpreted as the manifestation of a rather weak ordering of the charge with a checkerboard pattern. *COM* results manage to reproduce such double peak structure showing a capability to quantitatively describe, also in a translational invariant phase, rather strong charge correlations.

In Figs. 11 and 12, we report the behavior of $N(r)$, as a function of the distance $r = \sqrt{i^2 + j^2}$, for $U = 4$ and 12 , $T = 0.01$ and $n = 8/9$ and $U = 8$, $T = 0.25$ and $n = 0.2$, respectively. *COM* results are in good quantitative agreement with the numerical results^{7,8} showing once more that the charge dynamics is really well described by our solution. In Fig. 13, $N(i, i^{\alpha x})$ is shown as a function of the Coulomb repulsion U for $n = 8/9$ and $T = 0$. The

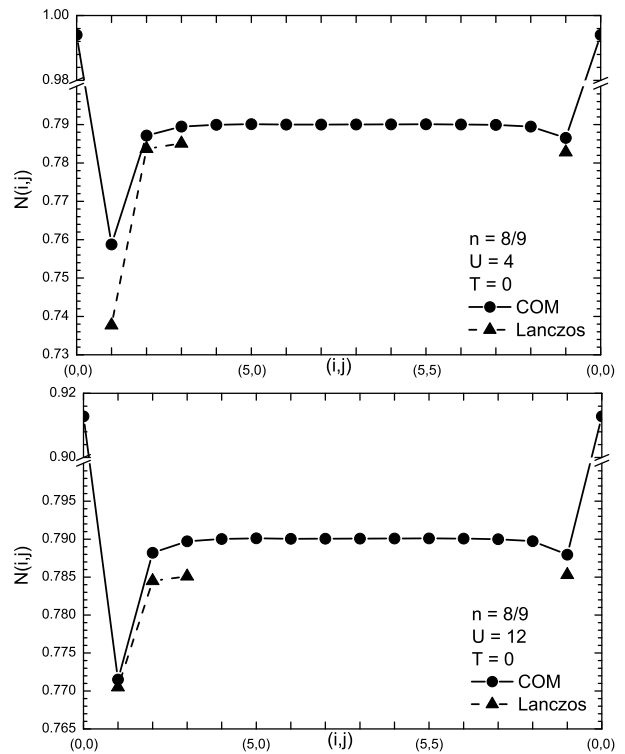


FIG. 12: The charge correlation function $N(r)$ as a function of the distance for $n = 8/9$, $U = 4$ (top) [$U = 12$ (bottom)] and $T = 0$; the Lanczos data (4×4) are from ? .

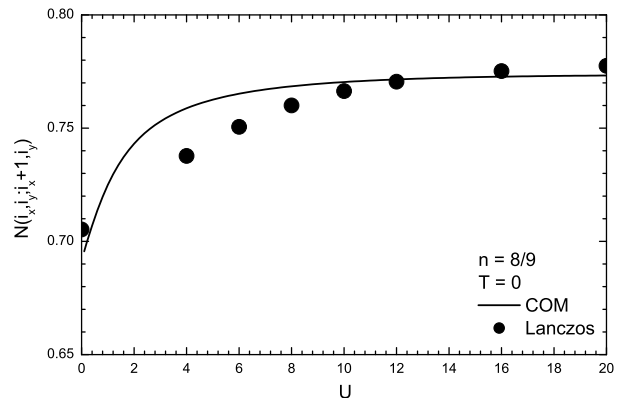


FIG. 13: The charge correlation function $N(i, i^{\alpha x})$ as a function of U for $n = 8/9$ and $T = 0$; the Lanczos data (4×4) are from ? .

agreement with Lanczos data⁷ is quite good and gets better and better as U increases.

V. CONCLUSIONS

An analytical description of the charge and spin dynamics of the two-dimensional Hubbard model in the

paramagnetic phase has been presented within a two-pole approximation in the framework of the *COM*. The hydrodynamics constraints as well as the Pauli principle requirements have been embedded in the fully self-consistent solution by the very beginning and any decoupling has been avoided. The antiferromagnetic correlations are really well described together with some weak charge ordering tendency at commensurate filling. Spin spectrum, static uniform spin susceptibility, spin and charge correlation functions are in very good agreement with the numerical results present in the literature and clearly state the reliability of the proposed procedure.

Acknowledgments

V.T. wishes to thank all the members of the Dipartimento di Fisica “E.R. Caianiello”, Università degli Studi di Salerno, and especially Prof. F. Mancini, for the kind hospitality.

APPENDIX

We have the following expressions for the $m^{(\mu)}$ -matrix entries

$$I_{l_\mu \rho_\mu}(\mathbf{k}) = \frac{3}{4} [1 - \alpha(\mathbf{k})] (12C^\alpha + C^\lambda + 6C^\mu) - \frac{3}{4} [1 - \eta(\mathbf{k})] (C^\alpha + C^\lambda + 2C^\mu) + \frac{1}{4} [1 - \lambda(\mathbf{k})] C^\lambda + \frac{3}{2} [1 - \mu(\mathbf{k})] C^\mu - 3 [1 - \beta(\mathbf{k})] (C^\alpha + C^\mu) \quad (1)$$

$$I_{\kappa_\mu \rho_\mu}(\mathbf{k}) = -2 [1 - \alpha(\mathbf{k})] D + [1 - 2\alpha(\mathbf{k})] (2E^\beta + E^\eta) + \eta(\mathbf{k}) E^\eta + 2\beta(\mathbf{k}) E^\beta + [1 - 2\alpha(\mathbf{k})] a_\mu + \frac{1}{4} [b_\mu + 2\beta(\mathbf{k}) c_\mu + \eta(\mathbf{k}) d_\mu] \quad (2)$$

The following definitions have been used

$$C^\alpha = \langle c^\alpha(i) c^\dagger(i) \rangle \quad (3)$$

$$C^\lambda = \langle c^\lambda(i) c^\dagger(i) \rangle \quad (4)$$

$$C^\mu = \langle c^\mu(i) c^\dagger(i) \rangle \quad (5)$$

$$E^\beta = \langle c^\beta(i) \eta^\dagger(i) \rangle \quad (6)$$

$$E^\eta = \langle c^\eta(i) \eta^\dagger(i) \rangle \quad (7)$$

$$a_\mu = 2 \langle c^\dagger(i) \sigma_\mu c^\alpha(i) c^\dagger(i) \sigma_\mu c^\alpha(i) \rangle - \langle c^{\alpha\dagger}(i) \sigma_\mu \sigma^\lambda \sigma_\mu c^\alpha(i) n_\lambda(i) \rangle \quad (8)$$

$$b_\mu = 2 \langle c^\dagger(i) \sigma_\mu c^\dagger(i) \sigma_\mu [c(i) c(i)]^\alpha \rangle - \langle c^\dagger(i) \sigma_\mu \sigma^\lambda \sigma_\mu c(i) n_\lambda^\alpha(i) \rangle \quad (9)$$

$$c_\mu = 2 \langle c^\dagger(i) \sigma_\mu c^\dagger(i^\eta) \sigma_\mu c(i^\alpha) c(i^\alpha) \rangle - \langle c^\dagger(i) \sigma_\mu \sigma^\lambda \sigma_\mu c(i^\eta) n_\lambda(i^\alpha) \rangle \quad (10)$$

$$d_\mu = 2 \langle c^\dagger(i) \sigma_\mu c^\dagger(i^\beta) \sigma_\mu c(i^\alpha) c(i^\alpha) \rangle - \langle c^\dagger(i) \sigma_\mu \sigma^\lambda \sigma_\mu c(i^\beta) n_\lambda(i^\alpha) \rangle \quad (11)$$

where we used the notation

$$i = (i_x, i_y, t) \quad (12)$$

$$i^\alpha = (i_x + a, i_y, t) \quad (13)$$

$$i^\eta = (i_x + 2a, i_y, t) \quad (14)$$

$$i^\beta = (i_x + a, i_y + a, t) \quad (15)$$

The functions β_{ij} , η_{ij} , μ_{ij} and λ_{ij} , the projectors on the second, third, fourth and fifth nearest neighbors, respectively, have the following expressions in momentum space

$$\beta(\mathbf{k}) = \frac{1}{2} \{ \cos[a(k_x + k_y)] + \cos[a(k_x - k_y)] \} \quad (16)$$

$$\eta(\mathbf{k}) = \frac{1}{2} [\cos(2a k_x) + \cos(2a k_y)] \quad (17)$$

$$\mu(\mathbf{k}) = \frac{1}{4} \{ \cos[a(2k_x + k_y)] + \cos[a(k_x + 2k_y)] + \cos[a(2k_x - k_y)] + \cos[a(k_x - 2k_y)] \} \quad (18)$$

$$\lambda(\mathbf{k}) = \frac{1}{2} [\cos(3a k_x) + \cos(3a k_y)] \quad (19)$$

The following relations hold

$$c^{\alpha^2}(i) = \frac{1}{4} [c(i) + 2c^\beta(i) + c^\eta(i)] \quad (20)$$

$$c^{\alpha^3}(i) = \frac{1}{16} [9c^\alpha(i) + c^\lambda(i) + 6c^\mu(i)] \quad (21)$$

* E-mail: avella@sa.infn.it

† E-mail: mancini@sa.infn.it

‡ Current address: CFIF, Instituto Superior Tecnico Av. Rovisco Pais, 1049-001 Lisbon, Portugal